

New prospects in studying Li diffusion – two-time stimulated echo NMR of spin-3/2 nuclei

Martin Wilkening^{*}, Paul Heitjans¹

*Institut für Physikalische Chemie und Elektrochemie, Universität Hannover, Callinstraße
3-3a, 30167 Hannover, Germany*

Abstract

The measurement of diffusion parameters like activation energies and translational jump rates of small cations plays a key role in materials science. Especially the in-depth investigation of Li diffusion in ionic conductors is of great interest, because suitable ionic conductors are needed for, e. g., the development of new secondary ion battery systems. As the standard tracer method is not applicable to study Li diffusion due to the lack of a suitable radioactive isotope, Li diffusion is alternatively probed by solid state NMR techniques. With the different NMR methods being available, diffusion processes can be studied on different length- and time-scales. In the present paper we use two-time spin-alignment echo (SAE) NMR for the direct, i. e., model independent, measurement of extremely small translational Li jump rates. To this end, different crystalline and glassy ion conductors like Li_xTiS_2 , Li_4SiO_4 as well as LiNbO_3 served as model substances to reveal the special features of this technique. SAE-NMR, which was originally developed for deuterons, has also been applied in a few cases to spin-3/2 nuclei, like ^7Li , before. The corresponding correlation functions yield not only information about diffusion parameters but also about geometric properties of the diffusion pathways, making SAE NMR a powerful method which complements well-established NMR techniques.

Key words: solid state NMR, Li diffusion, spin-alignment echoes, extremely slow motions

1 Introduction

Since its discovery exactly 60 years ago, nuclear magnetic resonance (NMR) spectroscopy has become a most powerful tool to investigate structure and dynamics in condensed matter. NMR spectroscopy has found extensive application also in the field of solid ionic conductors (see, e. g., Refs. [1,2]). Diffusion studies are especially common for ${}^7\text{Li}$ because of the often great mobility of lithium cations in a wide range of materials and the ease of observation of this (quadrupole) nucleus. Moreover, NMR is widely used to determine Li transport properties due to the fact that the standard tracer diffusion method is not applicable as no suitable radioactive Li isotope is available. In most of the NMR studies spin-lattice relaxation rates T_1^{-1} and the overall ${}^7\text{Li}$ linewidth versus temperature T were measured [1,3]. However, NMR spectroscopy offers a much larger set of various experiments with their advantages and disadvantages in probing ionic motions on different length- and time-scales [2,4]. In particular, frequency dependent relaxation measurements yield information about the dimensionality of the diffusion process under investigation [5].

Although classical relaxation NMR can be applied easily to a large variety of ma-

* Corresponding author. Fax: +49 511 762 19121.

E-mail address: wilkening@pci.uni-hannover.de

¹ Also for correspondence. Fax: +49 511 762 19121.

E-mail address: heitjans@pci.uni-hannover.de

URL: www.unics.uni-hannover.de/pciheitjans/akhei.html

materials and is able to reveal a great deal about Li dynamics over wide ranges of temperature [5–7], the interpretation of relaxation data is theoretically complex and, thus, oftentimes not independent of the theoretical model used for the correlation of experimental data with microscopic diffusion parameters. However, a relatively model-independent determination of jump rates is possible, if the maximum of the diffusion induced $T_1^{-1}(1/T)$ peak at a given Larmor frequency can be recorded. Whereas spin-lattice relaxation rates T_1^{-1} in the laboratory frame are sensitive to jump rates in the region of the ${}^7\text{Li}$ Larmor frequency being of the order of several hundreds MHz, slower ionic motions with jump rates between 10^6 s^{-1} and 10^4 s^{-1} can be probed by recording spin-lattice relaxation rates $T_{1\rho}^{-1}$ in the rotating frame [8]. However, one has to keep in mind that particularly at low temperatures other relaxation mechanisms or local (within-site) cation motions can dominate spin-lattice relaxation. These effects have almost no importance for long-range diffusion or conductivity.

In general, solid echo NMR spectroscopy, i. e., the measurement of transverse relaxation times T_2 , can reveal information about ionic motions with jump rates in the kHz range, depending on the modulation of interactions between the nucleus and the surrounding magnetic and/or electric fields through the dynamic process, see, e. g., Ref. [9]. Extraction of data relevant for long-range diffusion is difficult, once again. Furthermore, ionic motions on the ultra-slow time-scale, i. e., in the Hz to sub-Hz range, are usually not accessible because they do not affect the lineshape at all.

In the present work newly established stimulated echo ${}^7\text{Li}$ NMR methods are used to enable the *direct*, i. e., model-independent, access to microscopic Li diffusion parameters. Furthermore, stimulated echo NMR allows the measurement of extremely slow Li jumps with rates in the kHz to sub-Hz range. Recently, also 2D exchange

^6Li and ^7Li NMR experiments were used for the study of Li jump rates in the kHz range very successfully [10–12]. To our knowledge, so far only these few magic angle spinning (MAS) 2D exchange NMR experiments have been carried out to detect Li jumps between crystallographic distinct sites. 2D exchange NMR is applicable if a direct exchange process of Li nuclei between different sites becomes visible in the 2D NMR spectra, which could be due to different chemical shift or hyperfine interactions of the Li nuclei. Stimulated echo NMR, however, is applicable to a much broader class of crystalline and even amorphous materials. With the spin-alignment echo (SAE) technique, originally developed for deuterons (spin-1 nuclei) by Spiess [13], the spins are labeled by the interaction of the nucleus with a non-vanishing electric field gradient (EFG), produced by the distribution of electric charge carriers in the neighborhood of the nuclei. Deuteron SAE-NMR evolved into a powerful technique to precisely study the dynamics as well as geometric aspects of diffusion processes. Quite recently, stimulated echo NMR was also used to study successfully Ag dynamics, using the spin-1/2 nucleus ^{109}Ag , in crystalline and glassy materials [14–16].

The present work is part of the on-going effort to apply the SAE technique systematically to spin-3/2 nuclei, like ^7Li , with quadrupole couplings comparable to that of deuterons. The method has been applied before to detect ultraslow Be jumps in glasses [17–19] and also used to investigate Li diffusion in various crystalline ionic conductors [20–25]. However, a comprehensive comparison of ^7Li SAE-NMR results with data from 2D exchange NMR experiments and/or conventional relaxation NMR measurements, as presented here, is still missing. ^7Li spin-alignment echoes can be sampled with a common solid state NMR setup employing the Jeener-Broekaert sequence $90^\circ_x - t_p - 45^\circ_y - t_m - 45^\circ - t$, cf. Refs. [26,27]. Jumping of the ion between sites j and k with different (angular) quadrupole frequencies ω_{Q_j} and

ω_{Q_k} causes a time-dependence of ω_Q and thus leads to an echo decay from an initial echo amplitude at $t_m = 0$ to a final state amplitude at $t_m \gg 0$. In this way, for fixed evolution time t_p and variable mixing time t_m ($10 \mu\text{s} \leq t_m \leq 100 \text{s}$), an ensemble averaged two-time single-particle correlation function $S_2(t_m)$ of the ion hopping process can be recorded [27], giving (in the ideal case) direct access to the jump rate τ^{-1} . In order to suppress the creation of dipolar contributions simultaneously with the generation of quadrupolar order, in the case of ${}^7\text{Li}$ SAE-NMR sufficiently short evolution times $t_p < 20 \mu\text{s}$ have to be used to record two-time correlation functions [21,22,19]. This is in contrast to stimulated echo NMR of ${}^9\text{Be}$ being subject to relatively weak dipolar interactions.

2 Case studies

2.1 Li diffusion in lithium titanium disulfide

Up to now, we used a number of crystalline and amorphous (glassy) materials, which serve as model substances to study the potential of recording Jeener-Broekaert echoes [28]. For instance, the Li diffusion process in polycrystalline layered Li_xTiS_2 (CdI_2 structure, space group $P\bar{3}m1$, $0 < x \leq 1$) was investigated on different time-scales in a comprehensive study by classical spin-spin (T_2) and diffusion induced spin-lattice relaxation NMR in the laboratory (T_1) as well as in the rotating frame ($T_{1\rho}$) on the one hand, and stimulated-echo NMR on the other hand. Layered Li_xTiS_2 served as a singularly well-defined fast Li conductor [29,30] for the study of cation translational diffusion being confined to two dimensions [31], i. e., in the planes between the TiS_2 layers. In the present paper we focus on the compound with $x = 0.7$. A similar study of Li diffusion in layered Li_xTiS_2 with $x = 1.0$ has been

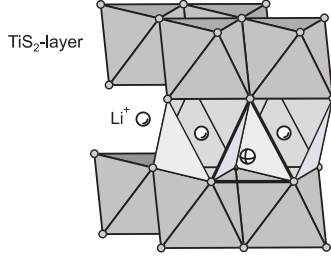


Fig. 1. Crystal structure of Li_xTiS_2 (space group $P\bar{3}m1$). A Li ion temporarily occupying a tetrahedral site between two neighbouring octahedra is also shown.

already presented by us in Ref. [24]. The crystal structure of Li_xTiS_2 is depicted in Fig.1. Li ions preferentially reside on octahedral sites within the TiS_2 layers [32]. No staging effects are known for Li_xTiS_2 . In Fig. 2 the decay of spin-alignment echo amplitudes $S_2(t_m)$ with increasing mixing time t_m is shown. Echoes were read out at $t = t_p$ with fixed evolution time t_p . The echo decay can be clearly subdivided into two parts and parameterized with a combination of two exponentials. At relatively long evolution times ($t_p = 75 \mu\text{s}$) the first decay step follows a single-exponential, $S_2 \propto \exp(-(t_m/\tau))$, whereas at short evolution times ($t_p = 15 \mu\text{s}$) a

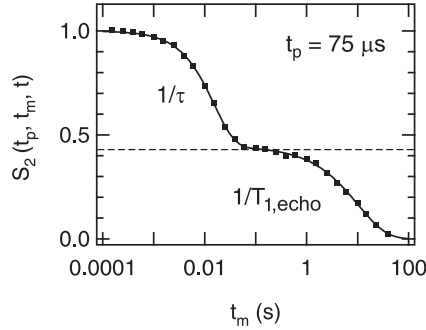


Fig. 2. Semilog plot of normalized spin-alignment echo (SAE) amplitudes $S_2(t_p, t_m, t = t_p)$ of $\text{Li}_{0.7}\text{TiS}_2$ at 188 K as a function of mixing time t_m (echoes were recorded after extensive phase cycling, amplitudes were read out at fixed evolution time $t = t_p = 75 \mu\text{s}$). The first decay step yields directly the Li residence time $\tau = 1.55(3) \times 10^{-2}\text{s}$, whereas the second decay step simply reflects decay of spin-order due to relaxation processes with $T_{1,\text{echo}}^{-1}$ of the order of 10 s^{-1} . The solid line represents a fit according to a combination of two exponentials.

stretched exponential, $S_2 \propto \exp(-(t_m/\tau)^\gamma)$, with $\gamma \approx 0.8$ is obtained. Presumably, dipolar interactions contribute to the correlation function at longer t_p [21], so that its non-exponential decay behaviour is increasingly masked with increasing evolution time. However, this influence on τ^{-1} is small, because the decay constant is nearly independent of the evolution time between $t_p = 10 \mu\text{s}$ and $t_p = 150 \mu\text{s}$. In this region the echo damping directly yields the Li jump rate τ^{-1} . The second decay is simply due to spin-lattice relaxation. Its decay constant is designated here as $T_{1,\text{echo}}^{-1}$, here. The window to measure jump rates τ^{-1} by SAE-NMR is given by the spin-spin relaxation rate T_2^{-1} and the spin-lattice relaxation rate T_1^{-1} as the upper and lower limit, respectively. In the samples investigated here, the rigid lattice value of T_2 is about $100 \mu\text{s}$. T_1 is of the order of $T_{1,\text{echo}}$ ranging between 8.8 and 19.9 s (220 K to 150 K). Therefore, ultra-slow Li jumps in the kHz to sub-Hz range can be detected by recording two-time spin-alignment echoes. The jump rates can be easily transformed into diffusion coefficients D according to $D = a^2/(2d \cdot \tau)$, when the dimensionality d of the diffusion process and the jump distance a are known. Li diffusion in Li_xTiS_2 is two-dimensional, which was unambiguously shown by the frequency and temperature dependence of NMR spin-lattice relaxation rates [31,33]. a is given by the distance between Li ions in octahedral and tetrahedral sites, as this is the dominant mechanism of Li diffusion in a sample with $x = 0.7$ (see below). The so obtained diffusion coefficients and the corresponding jump rates obtained by SAE-NMR at $t_p = 15 \mu\text{s}$ are shown in the Arrhenius representation of Fig. 3 (see also Fig. 1 in Ref. [25]). To confirm that SAE decay constants can be identified with microscopic Li jump rates, τ^{-1} values obtained via ^7Li NMR relaxation measurements in the laboratory and rotating frame are shown for comparison, too. The latter ones were determined via the maximum positions of the corresponding diffusion induced relaxation peaks $T_1^{-1}(1/T)$, which were recorded for different angular Larmor and locking frequencies, respectively [33,28]. Taken together, the

jump rates from the different methods obey an Arrhenius law with an activation energy of 0.41(1) eV and a preexponential factor of $6.3(1) \times 10^{12} \text{ s}^{-1}$, being of the order of phonon frequencies. The activation energy is in good agreement with values found in the literature [34,35] from macroscopic methods. Interestingly, by combining these quite different NMR techniques one and the same lithium diffusion process was probed over a dynamic range of almost 10 orders of magnitude with jump rates (cf. Fig. 3) between $1 \times 10^{-1} \text{ s}^{-1}$ and $7.8 \times 10^8 \text{ s}^{-1}$ (148 – 510 K).

In addition to the direct measurement of ultra-slow Li jump rates, SAE-NMR in general serves as a tool for the investigation of geometric properties of diffusion pathways [15,36]. The first decay step of the two-time correlation function of Fig. 2 leads to a final state amplitude S_∞ of about 0.42 (dashed line in Fig. 2) at intermediate t_m of about 0.1 s. For sufficiently long evolution times, S_∞ will attain the limiting value $1/N$, where N is the number of (equally populated) distinct sites visited by the jumping ion. Thus, S_∞ is similar to the elastic incoherent structure factor

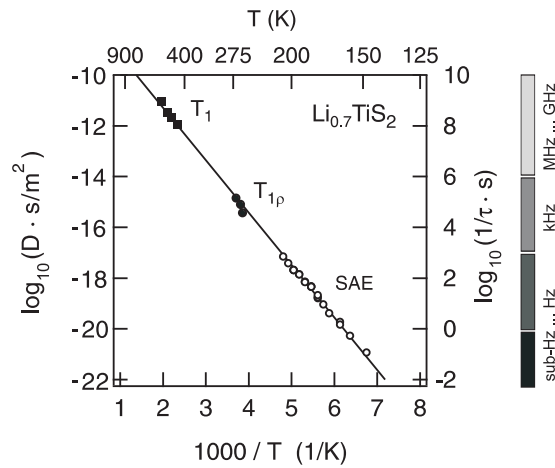


Fig. 3. Probing Li diffusion in $\text{Li}_{0.7}\text{TiS}_2$ on different time-scales: Comparison of jump rates obtained directly by SAE-NMR (\circ) with those deduced from the diffusion induced maxima of the $1/T_{1(\rho)}(1/T)$ -peaks at different Larmor (\blacksquare , 10...77 MHz) and locking frequencies (\bullet , 2.1...10 kHz). The straight line represents an activation energy of 0.41(1) eV.

(EISF) in neutron scattering. The evolution of S_∞ as a function of t_p is shown in Fig. 4, indicating clearly a two-site jump process between the two only possible Li sites in Li_xTiS_2 . Obviously, Li ions jump between equivalent octahedral sites with the tetrahedral site as transitional position (Fig. 1), having a different electric field gradient [37]. Although Li ions occupy preferentially octahedral sites in Li_xTiS_2 , the tetrahedral position is visited in each individual hopping process, so that $N = 2$ different quadrupole frequencies are involved in the diffusion process, disregarding the different occupancy of the two sites.

The echo amplitude S_2 would not decay according to a two-step behaviour, if the Li ions jump between two octahedral positions directly. In such a case ω_Q would not change, and the echoes would be simply damped by relaxation processes, only. In Li_xTiS_2 with its two distinct Li positions, a two-step behaviour of the correlation function is only consistent with a final state amplitude $S_\infty(t_p \rightarrow \infty)$ of $1/2$. Thus, ^7Li SAE-NMR is well able to determine both the dynamics and the geometry of a given diffusion process. The diffusion pathway found here is in agreement with theoretical calculations on Li_xTiS_2 [38] as well as on isostructural Li_xTiSe_2 [39].

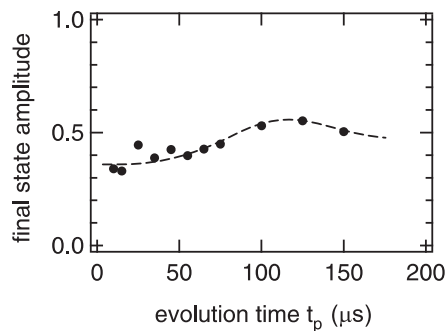


Fig. 4. Evolution of final state amplitudes S_∞ with increasing t_p . S_∞ values were obtained from two-time correlation functions S_2 recorded at a frequency of 155 MHz and at $T = 188$ K. The dashed line is just to guide the eye.

2.2 *Slow Li exchange in lithium orthosilicate*

The low-temperature modification of lithium orthosilicate Li_4SiO_4 served as another interesting model case for the demonstration of stimulated-echo NMR spectroscopy as to be, besides 2D MAS-NMR, a complementary tool for the investigation of slow Li dynamics in crystalline Li conductors. Polycrystalline Li_4SiO_4 is interesting with respect to SAE-NMR because of the presence of a relatively large number of electrically inequivalent sites for Li cations. At low temperatures the high-resolution ^6Li MAS-NMR spectrum is composed of four resolved or partially resolved peaks [40] due to Li in distorted three-, four-, five-, and six-fold coordination in agreement with the crystal structure. The Li^+ exchange process between these different crystallographic sites was observed via recording temperature dependent 1D ^6Li MAS spectra by Stebbins et al. [40]. At the coalescence temperature of 363 K an overall jump rate of about $300 \pm 100 \text{ s}^{-1}$ was estimated by the authors. Additionally, lithium dynamics in Li_4SiO_4 was probed directly by 2D exchange NMR spectroscopy by the Stebbins group [10]. In this pioneering work on the detection of Li exchange processes in solid ion conductors, 2D spectra were recorded at two different temperatures and two different mixing times in each case.

Motivated by this work, we have studied the lithium diffusion in polycrystalline Li_4SiO_4 by two-time ^7Li stimulated echo NMR spectroscopy at different Larmor frequencies. Slow Li motions were monitored between 300 K and 433 K by recording spin-alignment echoes at short evolution times $t_p = 10 \mu\text{s}$ as a function of t_m (Fig. 5). Similar to the case of Li_xTiS_2 , the decay curves show biexponential behaviour in this temperature range and can be fitted with a combination of two stretched exponentials. The arrow in Fig. 5 indicates the beginning of the second decay step. The echo amplitudes of the first decay step follow the stretched expo-

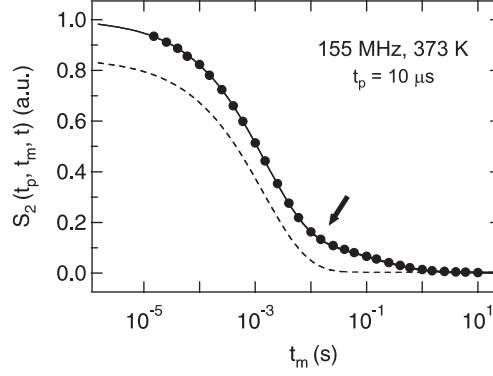


Fig. 5. Typical SAE amplitudes S_2 of Li_4SiO_4 at $t_p = 10 \mu\text{s}$ vs t_m at 373 K. The echo decay proceeds in two steps: The first decay step reflects slow Li jumps between different sites in Li_4SiO_4 ; whereas the second one is presumably due to spin-lattice relaxation. The dashed line represents the correlation function after correcting for the contribution by spin-lattice relaxation which is reflected by the second decay step.

ponential $S_2(t_m) \propto \exp(-(t_m/\tau)^\gamma)$. The stretching exponent decreases from 0.7 to 0.4 with the temperature increasing from 300 K to 433 K. The decrease of γ might be the consequence of dipolar contributions being averaged with increasing temperature. These contributions seem to increase the τ^{-1} values by a factor of two, if at all, as has been shown in detail in Ref. [28].

Whereas the first decay step of the S_2 -curve in Fig. 5 reflects directly ionic jumps, the second one is due to the decay of echo intensity because of spin-lattice relaxation effects. The temperature dependent decay constants τ^{-1} ($10 \text{ s}^{-1} \leq \tau^{-1} \leq 2000 \text{ s}^{-1}$) show Arrhenius behaviour with an activation energy of 0.53(1) eV (Fig. 6). As expected for jump rates, the measured τ^{-1} values are independent of the Larmor frequency (32 – 155 MHz) used to measure the alignment decay. The τ^{-1} values from ^7Li SAE-NMR are in very good agreement with those obtained by two-dimensional ^6Li exchange MAS-NMR by Xu et al. [10] (cf. Fig. 6). For instance, from the ^7Li SAE-NMR decay at 363 K ($t_p = 10 \mu\text{s}$) a Li jump rate of 380 s^{-1} is obtained (see Fig. 6). The 2D exchange rates shown in Fig. 6 represent the sum of

Li jumps between $\text{LiO}_4 \leftrightarrow \text{LiO}_3$, $\text{LiO}_4 \leftrightarrow \text{LiO}_6$, $\text{LiO}_5 \leftrightarrow \text{LiO}_6$, as well as between $\text{LiO}_3 \leftrightarrow \text{LiO}_6$ polyhedra. A final state amplitude S_∞ of about 0.23(2) at 433 K correctly indicates already at a rather short evolution time that four to five Li sites are involved in the diffusion process. In general, final state amplitudes containing geometric information have to be sampled at large t_p . However, in the case of Li_4SiO_4 the amplitude S_∞ decreases with increasing t_p [28]. For example, at $t_p = 100 \mu\text{s}$ the plateau value S_∞ is decreased to about 0.1. In the case of ^7Li the final state amplitude is additionally affected by the number of dipolarly coupled ^7Li spins [22]. The more spins are effectively coupled, and this might be the case at large evolution times in Li_4SiO_4 , the smaller becomes the plateau value S_∞ .

It was also concluded from 2D exchange NMR that all Li sites participate in the transport process [10]. Jumps between LiO_5 and LiO_4 polyhedra which were not quantitatively detected by 2D exchange NMR seem to be of minor importance for the diffusion process.

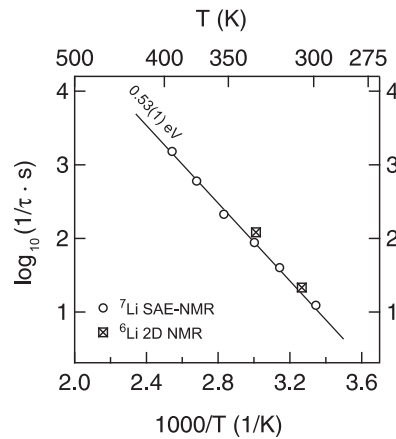


Fig. 6. Comparison of jump rates recorded directly by ^7Li SAE-NMR at 155 MHz and $t_p = 10 \mu\text{s}$ with those extracted from ^6Li 2D exchange NMR experiments carried out by Xu et al. [10] at 58 MHz and two different temperatures. The 2D exchange rates are each afflicted with a sampling error of about 10%. Independent of the Li isotope and, of course, of the frequency, nearly the same results were found.

2.3 Li diffusion in amorphous lithium niobate

In contrast to crystalline materials with a finite number of different electrically inequivalent sites, in amorphous (or glassy) materials with their infinite number of slightly different sites the echo amplitudes $S_2(t_m)$ decay to zero with increasing mixing time. ^7Li SAE-decay curves of amorphous LiNbO_3 are shown in Fig. 7.

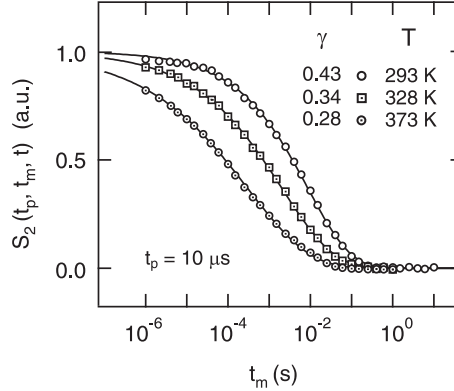


Fig. 7. Two-time hopping correlation functions $S_2(t_p, t_m, t = t_p)$ of LiNbO_3 recorded at $t_p = 10 \mu\text{s}$ and different temperatures T . The exponent γ is not independent of temperature but decreases with increasing T .

The amorphous sample was prepared via sol-gel synthesis. Details of the sample preparation are given elsewhere [41]. As in the case of Li_4SiO_4 , the echo decay can be fitted with a stretched exponential and the stretching exponent γ varies with temperature T (cf. listed values in Fig. 7). Once again, the non-exponentiality of the correlation functions is increasingly masked by dipolar contributions to the stimulated echo. Spin-lattice relaxation proceeds on a much longer time scale and has no influence on the echo damping. In the investigated temperature range the rates T_1^{-1} take values between 10^0 s^{-1} and 10^{-1} s^{-1} at 155 MHz.

Strongly stretched hopping correlation functions might be the consequence of a distribution of jump rates in disordered materials and/or of an intrinsically non-

exponential decay function, e. g., due to the presence of correlated forward and backward jumps. However, it has recently been shown by ^{109}Ag NMR that non-exponential hopping correlation functions in glassy Ag ion conductors are due to the existence of a broad distribution of jump rates rather than to correlated back-and-forth jumps [16]. Moreover, molecular dynamics simulations of Li dynamics in LiPO_3 glass by Vogel [42] have shown that the probability of correlated back-and-forth jumps between neighboring sites is significantly reduced for the slow ions within a distribution of jump rates.

In Fig. 8 SAE decay rates τ^{-1} recorded at 77 and 155 MHz are shown vs $1/T$. As expected, τ^{-1} is also in this case independent of the resonance frequency, whereas the spin-lattice relaxation rate T_1^{-1} strongly depends on the Larmor frequency [41]. Between 293 K and 418 K the jump rates take values from 10^2 s^{-1} up to 10^4 s^{-1} . Arrhenius behaviour with an activation energy of 0.41(1) eV is found. Interestingly, this value is more comparable to activation energies which were reported from dc conductivity measurements (0.4 to 0.6 eV, cf. Refs. [43–45]) rather than to those

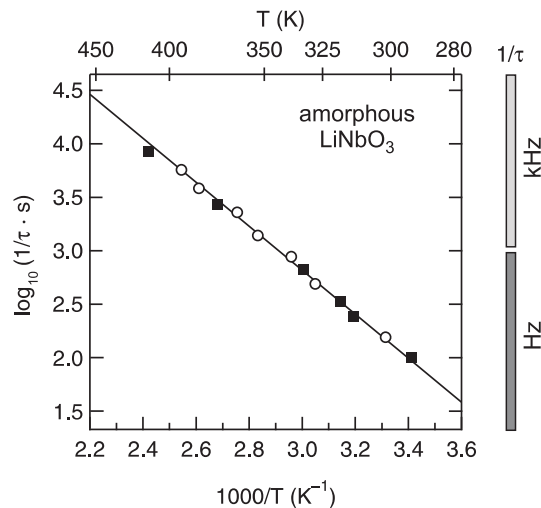


Fig. 8. ^7Li SAE echo decay rates τ^{-1} vs reciprocal temperature. Values were recorded at two different magnetic fields corresponding to resonance frequencies of 77 MHz (■) and 155 MHz (○). As expected for a motional correlation time, τ is field-independent.

which can be obtained from the low-temperature flank of the NMR spin-lattice relaxation peak $T_1^{-1}(1/T)$. The latter measurements yield an activation energy of about 0.25 eV [41]. However, this value is not in contradiction to the one from SAE-NMR, as the low- T flank of the $T_1^{-1}(1/T)$ peak is influenced by short-range Li diffusion [5]. Furthermore, correlation effects due to Coulomb interactions and structural disorder will additionally reduce the slope of the low- T flank resulting in an apparent activation energy of about 0.25 eV. Unfortunately, neither the high- T flank of the $T_1^{-1}(1/T)$ peak nor the maximum of this peak can be reached experimentally due to the heat-sensitivity of amorphous LiNbO_3 . Experiments have to be restricted to below 450 K in order to avoid crystallization. This is in contrast to the NMR studies performed on Li_xTiS_2 which is stable up to very high-temperatures. The slope of the high- T flank of the peak $T_1^{-1}(1/T)$ would correspond to the activation energy describing the long-range Li transport in LiNbO_3 . This activation energy was predicted to be about 0.4 eV taking into account the frequency dependence of the diffusion induced T_1^{-1} rates on the low-temperature flank [41]. Thus, we can identify the value obtained by SAE-NMR with the activation energy of long-range Li transport in LiNbO_3 . This comparison makes SAE-NMR to be an interesting alternative to conventional NMR relaxation experiments as it does not require (extremely) high temperatures, so that temperature-sensitive materials with moderate Li diffusivities can be studied.

3 Conclusions

NMR spectroscopy offers a large set of experiments probing ionic motions on different time- and length-scales. In the present paper, we have used ^7Li spin-alignment echo NMR spectroscopy to enlighten Li dynamics in several Li ion conduc-

tors serving here as model substances. ^7Li SAE-NMR can be used for the *direct* measurement of microscopic diffusion parameters. Results were compared to those of conventional relaxation NMR, 2D exchange NMR, as well as to dc-conductivity data describing macroscopic transport, being found in the literature.

In the case of Li_xTiS_2 with $x = 0.7$, the mixing time dependent ^7Li SAE-decay was investigated over a dynamic range of about four decades. Directly obtained extremely slow jump rates are fully consistent with those obtained via recording diffusion induced spin-lattice relaxation peaks, probing Li dynamics on much shorter time-scales. Taken together, by the combination of these different NMR techniques, one and the same diffusion process was recorded over a dynamic range of about ten decades. The evolution time dependent measurements have demonstrated the potential of ^7Li SAE-NMR to study geometric details of a given diffusion process. We found large evidence for a two-site jump process in layer-structured $\text{Li}_{0.7}\text{TiS}_2$, being in agreement with theoretical predictions found in the literature.

In the case of Li_4SiO_4 , we have shown that SAE-NMR is a time-saving alternative to 2D exchange NMR. The main advantage over exchange NMR is the fact that it is applicable to a much broader class of crystalline and even amorphous materials because there is no need to record well-resolved Li spectra in order to quantify the exchange of Li ions between distinct sites.

The SAE-NMR measurements on amorphous LiNbO_3 pointed out the possibility to use ^7Li stimulated echo NMR for studying also heat-sensitive materials. In all cases activation energies were found to be in fair agreement with those obtained by macroscopic methods.

Altogether, ^7Li SAE-NMR is likely to become a powerful method which is able to complement other already well-established and sophisticated NMR techniques.

Acknowledgement

Financial support of the DFG (Deutsche Forschungsgemeinschaft) is gratefully acknowledged.

References

- [1] D. Brinkmann, *Prog. Nucl. Magn. Reson. Spectrosc.* 24 (1992) 527.
- [2] P. Heitjans, S. Indris, and M. Wilkening, *Diffusion Fundamentals* 2 (2005) 45; P. Heitjans, S. Indris, and M. Wilkening, in J. Kärger, P. Heitjans, and F. Grinberg, *Diffusion Fundamentals*, Leipziger Universitätsverlag, Leipzig 2005, p. 226.
- [3] P.M. Richards, in M.B. Salamon (Ed), *Topics in Current Physics*, Vol. 15, Springer, Berlin, 1979, p. 141.
- [4] P. Heitjans and J. Kärger (Eds), *Diffusion in Condensed Matter – Methods, Materials, Models*, Springer, Berlin, 2005.
- [5] P. Heitjans, A. Schirmer, and S. Indris, in P. Heitjans and J. Kärger (Eds.), *Diffusion in Condensed Matter – Methods, Materials, Models*, Springer, Berlin, 2005, p. 367.
- [6] D. Bork and P. Heitjans, *J. Phys. Chem. B* 105 (2001) 9162.
- [7] P. Heitjans and S. Indris, *J. Phys.: Condens. Matter* 15 (2003) R1257.
- [8] D.C. Ailion and C.P. Slichter, *Phys. Rev.* 137 (1965) A235.
- [9] M. Wagemaker, R. van de Krol, A.P.M. Kentgens, A.A. van Well and F.M. Mulder, *J. Amer. Chem. Soc.* 123 (2001) 11454.
- [10] Z. Xu and J.F. Stebbins, *Science* 270 (1995) 1332.
- [11] V.W.J. Verhoeven, I.M. de Scheper, G. Nachtegaal, A.P.M. Kentgens, E.M. Kelder, and F.M. Mulder, *Phys. Rev. Lett.* 86 (2001) 4314.

- [12] L.S. Cahill, R.P. Chapman, J.F. Britten, and G.R. Goward, *J. Phys. Chem. B* 110 (2006) 7171.
- [13] H.W. Spiess, *J. Chem. Phys.* 72 (1980) 6755.
- [14] M. Vogel, C. Brinkmann, H. Eckert, and A. Heuer, *Phys. Rev. B* 69 (2004) 094302.
- [15] C. Brinkmann, S. Faske, M. Vogel, T. Nilges, A. Heuer, and H. Eckert, *Phys. Chem. Chem. Phys.* 8 (2006) 369.
- [16] M. Vogel, C. Brinkmann C, H. Eckert, and A. Heuer, *Solid State Nucl. Magn. Res.* 22 (2002) 344.
- [17] X.-P. Tang, U. Geyer, R. Busch, W.L. Johnson, and Y. Wu, *Nature* 402 (1999) 160.
- [18] X.-P. Tang and Y. Wu, *J. Magn. Res.* 133 (1998) 155.
- [19] X.-P. Tang, R. Busch, W.L. Johnson, and Y. Wu, *Phys. Rev. Lett.* 81 (1998) 5358.
- [20] R. Böhmer, T. Jörg, F. Qi, and A. Titze, *Chem. Phys. Lett.* 316 (2000) 419.
- [21] F. Qi, T. Jörg, and R. Böhmer, *Solid State Nucl. Magn. Res.* 22 (2002) 484.
- [22] F. Qi, G. Diezemann, H. Böhm, J. Lambert, and R. Böhmer, *J. Magn. Res.* 169 (2004) 225.
- [23] F. Qi, C. Rier, R. Böhmer, W. Franke, and P. Heitjans, *Phys. Rev. B* 72 (2005) 104301.
- [24] M. Wilkening and P. Heitjans, *Defect Diffus. Forum* 237-240 (2005) 1182.
- [25] M. Wilkening and P. Heitjans, *Diffusion Fundamentals* 2 (2005) 60.
- [26] J. Jeener and P. Broekaert, *Phys. Rev.*, 157 (1967) 232.
- [27] R. Böhmer, *J. Magn. Reson.* 147 (2000) 78.
- [28] M. Wilkening, PhD thesis, University of Hannover, 2005.
- [29] M.S. Whittingham, R. Chen, T. Chirayil, and P. Zavalij, *Solid State Ion.* 94 (1997) 227.
- [30] M.S. Whittingham, *Prog. Solid State Chem.* 12 (1978) 41.
- [31] W. Küchler, P. Heitjans, A. Payer, and R. Schöllhorn, *Solid State Ion.* 70/71 (1994) 434.

- [32] J.R. Dahn, W.R. McKinnon, R.R. Haering, W.J.L. Buyers, and B.M. Powell, *Can. J. Phys.* 58 (1980) 207.
- [33] W. Kuchler, PhD thesis, University of Hannover, 1993.
- [34] K. Kanhehori, F. Kirino, T. Kudo, and K. Miyauchi, *J. Electrochem. Soc.*, 138 (1991) 2216.
- [35] A. Honders, *Solid State Ion.*, 15 (1985) 265.
- [36] T. Dries, F. Fujara, M. Kiebel, E. Rössler, and H. Silescu, *J. Chem. Phys.* 88 (1988) 2139.
- [37] T. Bredow, P. Heitjans, and M. Wilkening, *Phys. Rev. B* 70 (2004) 115111.
- [38] F. Mendizábal, R. Contreras, and A. Aizman, *J. Phys.: Condens. Mat.* 9 (1997) 3011.
- [39] C. Ramírez, R. Adelung, R. Kunz, L. Kipp, and W. Schattke, *Phys. Rev. B* 71 (2005) 035426.
- [40] J.F. Stebbins, Z. Xu, and D. Vollath, *Solid State Ion.*, 78 (1995) L1.
- [41] M. Wilkening, D. Bork, S. Indris, and P. Heitjans, *Phys. Chem. Chem. Phys.* 4 (2002) 3246.
- [42] M. Vogel, *Phys. Rev. B* 68 (2003) 184301.
- [43] P. Heitjans, M. Masoud, A. Feldhoff, and M. Wilkening, *Faraday Discuss.*, 2006, DOI:10.1039/B602887J.
- [44] M. Masoud and P. Heitjans, *Defect Diffus. Forum* 237-240 (2005) 1016.
- [45] A. Glass, K. Nassau, and T. Negran, *J. Appl. Phys.* 49 (1978) 4808.